Max-Planck-Institut für Plasmaphysik

EUROfusion

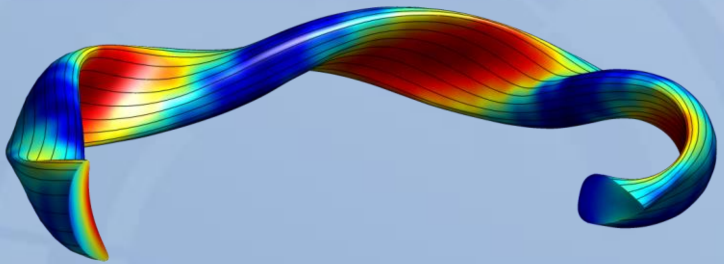

Impurity transport in stellarator plasmas

Albert Mollén

Max Planck Institute for Plasma Physics, Greifswald, Germany

Acknowledgements: M. Landreman, H. M. Smith, S. Buller, J. M. García-Regaña, J. L. Velasco, S. L. Newton, J. A. Alcusón, P. Xanthopoulos, A. Zocco, K. Aleynikova, M. Nunami, M. Nakata, A. Langenberg, P. Helander, The LHD experiment group and The Wendelstein 7-X Team*

***For the Wendelstein 7-X Team see author list of R. C. Wolf et al., Nucl. Fusion 57 (2017) 102020**

This work has been carried out within the framework of the EUROfusion Consortium and has received funding from the Euratom research and training programme 2014-2018 under grant agreement No 633053. The views and opinions expressed herein do not necessarily reflect those of the European Commission.

Outline

- Introduction to impurity transport in 3D plasmas
- Numerical tools and the SFINCS code
- Experimental observations of impurity transport
- Linear gyrokinetic modelling of impurity transport with equilibrium electrostatic potential variations
- Summary

Outline

- Introduction to impurity transport in 3D plasmas
- Numerical tools and the SFINCS code
- Experimental observations of impurity transport
- Linear gyrokinetic modelling of impurity transport with equilibrium electrostatic potential variations
- Summary

Neoclassical impurity accumulation is a concern for stellarators

- Impurity accumulation is a concern for stellarators,

  e.g. $\Rightarrow$ **radiation collapse**.

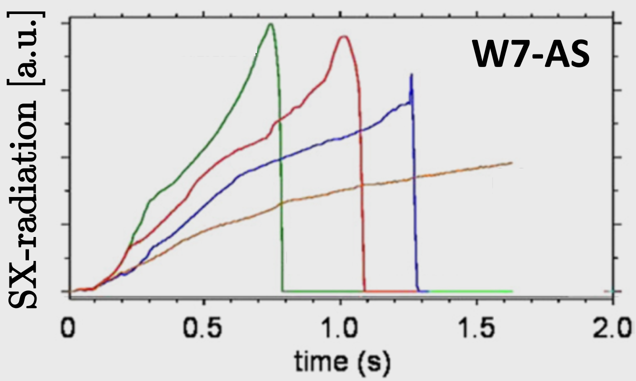

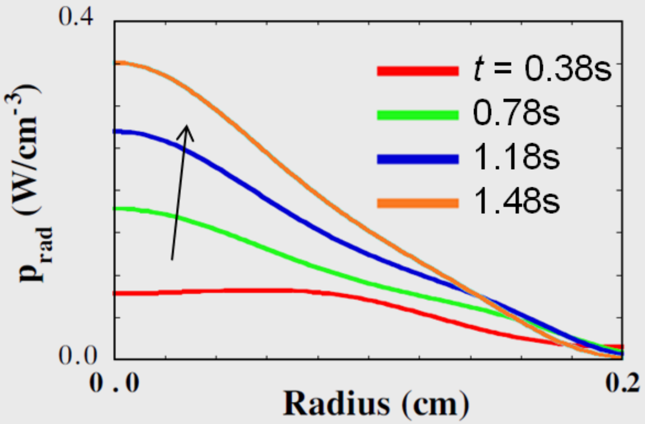

[Burhenn et al., Nucl. Fusion (2009)]
[Giannone et al., Plasma Phys. Control. Fusion (2000)]

- Neoclassical impurity accumulation predicted to be worse in stellarators than tokamaks:

  Radial electric field E_r often points inwards $\Rightarrow$ impurity accumulation.

- No Greenwald limit in stellarators, but density is limited by radiation from impurities.

Neoclassical impurity accumulation

In a tokamak (toroidal symmetry)

- The Lagrangian is independent of the toroidal angle. Additional constant of motion.
- The neoclassical particle fluxes are intrinsically ambipolar $\Rightarrow$ cross-field transport not affected by $E_r = -d\Phi/dr$ (except centrifugal and Coriolis forces if strong rotation).

Tokamak

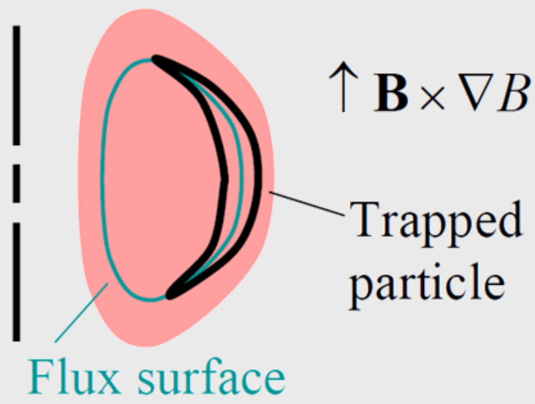

In a stellarator (broken toroidal symmetry)

- Helically trapped particles can drift out of the plasma $\Rightarrow$ collisionless trajectories can leave the confined region.
- $1/\nu$ - , $\sqrt{\nu}$ - regimes with enhanced neoclassical transport.
- Radial electric field E_r restores ambipolarity.
- E_r often points radially inwards $\Rightarrow$

Impurity accumulation.

Stellarator

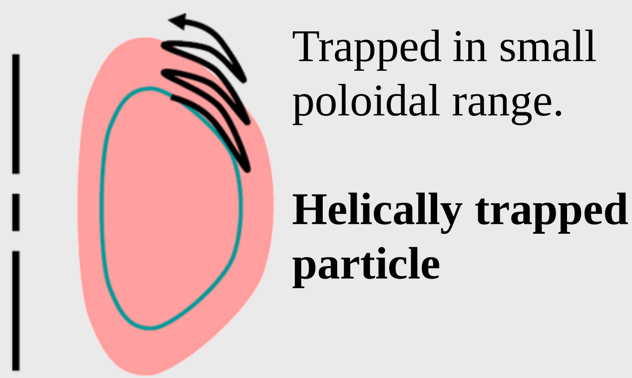

Temperature screening and the role of E_r in neoclassical transport

- The radial impurity flux can be written

$$\langle \Gamma_z \cdot \nabla r \rangle = L_{11}{}^{zz} A_{1z} + L_{11}{}^{zi} A_{1i} + L_{12}{}^{zz} A_{2z} + L_{12}{}^{zi} A_{2i}$$

"Thermodynamic forces"

$$A_{1a} = d(\ln p_a)/dr + (Z_a e/T_a)\; d\Phi/dr$$

$$A_{2a} = d(\ln T_a)/dr \qquad \text{(note: } T_z = T_i \text{)}$$

- **In a tokamak** E_r= - $d\Phi/dr$ has no effect on radial neoclassical transport.

$$\langle \Gamma_i \cdot \nabla r \rangle \simeq -Z\ \langle \Gamma_z \cdot \nabla r \rangle$$

Temperature screening of the impurities by the bulk ion temperature gradient can arise.

- **In a stellarator** E_r has a strong impact on the radial transport.

E_r determined from ambipolarity.

Temperature screening and the role of E_r in neoclassical transport

- **Conventional wisdom in stellarators** (from pitch-angle scattering models)

Intra-species terms ($L_{11}{}^{zz}$,$L_{12}{}^{zz}$) dominate over inter-species terms ($L_{11}{}^{zi}$,$L_{12}{}^{zi}$), i.e.

$$\langle\Gamma_z \cdot \nabla r\rangle \simeq L_{11}{}^{zz} d(\ln p_z)/dr + L_{11}{}^{zz}(Ze/T_z) d\Phi/dr + L_{12}{}^{zz} d(\ln T_z)/dr \,.$$

In ion root E_r is determined by ambipolarity from bulk-ion transport:

$$(e/T_i)\ d\Phi/dr = -\ d(\ln p_i)/dr - (L_{12}{}^{ii}/L_{11}{}^{ii})\ d(\ln T_i)/dr \,.$$

Substitute into impurity transport equation

$$\langle\Gamma_z \cdot \nabla r\rangle = L_{11}{}^{zz}[d(\ln p_z)/dr - Z\ \{d(\ln p_i)/dr + (L_{12}{}^{ii}/L_{11}{}^{ii})\ d(\ln T_i)/dr\}] + L_{12}{}^{zz}\ d(\ln T_z)/dr \,.$$

Coefficient in front of $d(\ln T_i)/dr$: $-Z\ L_{11}{}^{zz}(1 + L_{12}{}^{ii}/L_{11}{}^{ii})$ is always positive $\Rightarrow$

No temperature screening.

- **Conventional picture (all plasma species at low collisionality + pitch-angle scattering) successful in explaining experimental observations, with some notable exceptions:**

  - The carbon impurity hole in Large Helical Device. [Ida et al., Phys. Plasmas (2009)]

  - The high-density H-mode in Wendelstein 7-AS. [McCormick et al., Phys. Rev. Lett. (2002)]

- **In recent years a revived interest in neoclassical impurity physics, advances in analytical and numerical modeling:**

  - In high-collisionality regime $\nu_{*ii} = \nu_{ii}/\omega_{ti} \sim \nu_{ii}/v_{Ti} \gg 1$ (all ion species) the impurity transport is independent of E_r. [Braun & Helander, PoP (2010)]

  - Experimentally relevant mixed-collisionality transport regime, $\nu_{*zz} \gg 1;\ \nu_{*ii} \ll 1$, weak drive of impurity transport by E_r, ∇T_i -screening possible also in stellarators. [Helander et al., Phys. Rev. Lett. (2017)]

  - Effect of flux-surface potential variations $\Phi_1(\theta, \zeta) = \Phi - \langle\Phi\rangle$. [García-Regaña et al., PPCF (2013); Nucl. Fusion (2017); PPCF (2018)], [Mollén et al., PPCF (2018)], [Buller et al., J. Plasma Phys. (2018)]

  - Φ_1 + tangential magnetic drifts. [Velasco et al., PPCF (2018)], [Calvo et al., PPCF (2017); Nucl. Fusion (2018)]

Outline

- Introduction to impurity transport in 3D plasmas
- Numerical tools and the SFINCS code
- Experimental observations of impurity transport
- Linear gyrokinetic modelling of impurity transport with equilibrium electrostatic potential variations
- Summary

Numerical tools for calculating neoclassical transport in stellarators

- **DKES** [Hirshman et al., Phys. Fluids (1986)] (Drift Kinetic Equation Solver)

  - The main workhorse for neoclassical calculations in stellarators.

  - Radially local; mono-energetic, speed is a parameter $\Rightarrow$ 3D.

  - Pitch-angle scattering (momentum correction can be applied afterwards).

New codes start to explore extended physics (these are a few of them):

- **FORTEC-3D** [Satake et al., Plasma Fusion Res. (2008)]

  5D, radial coupling is retained.

- **EUTERPE** [García-Regaña et al., PPCF (2013); Nucl. Fusion (2017)]

  Radially local particle in cell Monte Carlo code. Pitch-angle scattering + momentum correction.

  Flux surface variations of electrostatic potential $\Phi_1(\theta, \zeta) = \Phi - \langle\Phi\rangle$.

- **SFINCS** [Landreman et al., Phys. Plasmas (2014), Mollén et al., PPCF (2018)]

  Radially local 4D, continuum code. Eulerian uniform grid in θ, ζ.

  Linearized Fokker-Planck collisions + Φ_1 + additional effects.

- **KNOSOS** [Velasco et al., PPCF (2018)]

  Orbit-averaged equation. Pitch-angle scattering. Φ_1 + tangential magnetic drifts.

Solves the time-independent radially local δf 4D drift-kinetic equation and calculates flows and radial fluxes, e.g. $$\langle \Gamma_s \cdot \nabla r \rangle = \langle \int d^3v f_{1s} (\mathbf{v}_{ds} + \mathbf{v}_E) \cdot \nabla r \rangle.$$

SFINCS can simultaneously take into account:

- Arbitrary number of kinetic species (non-trace impurities, non-adiabatic electrons).
- Full linearized Fokker-Planck collision operator.
- Self-consistent calculation of ambipolar E_r found by iterating until $\langle \mathbf{J} \cdot \nabla r \rangle = \sum_s Z_s e \langle \Gamma_s \cdot \nabla r \rangle = 0$.

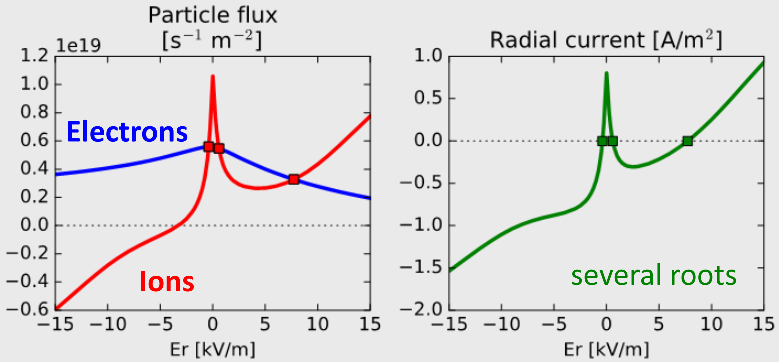

- Flux-surface potential variations

$\Phi_1(\theta, \zeta) = \Phi - \Phi_0(r)$; $\Phi_0(r) = \langle \Phi \rangle$; $\Phi_1 \ll \Phi_0$ $\Rightarrow$

$f_{1s}(\theta, \zeta, \xi, x)$, $\Phi_1(\theta, \zeta)$ unknowns $\Rightarrow$ nonlinear system of equations.

SFINCS available on: https://github.com/landreman/sfincs

[Landreman, Smith, Mollén & Helander, Phys. Plasmas (2014)]

Drift-kinetic equation that SFINCS solves

$$\begin{cases} \dot{\mathbf{R}} = v_\parallel \mathbf{b} - (\nabla\Phi_0 \times \mathbf{b})/B \\ \dot{v}_\parallel = - Z_s e \mathbf{b}\cdot\nabla\Phi_1/m_s - \mu \mathbf{b}\cdot\nabla B - v_\parallel (\mathbf{b}\times\nabla B)\cdot\nabla\Phi_0/B^2 \\ \dot{\mu} = 0 \\ f_{0s} = f_{Ms} \exp(-Z_s e \Phi_1/T_s) \end{cases}$$

occurrence of Φ_1 in red

$$\dot{\mathbf{R}}\cdot\nabla f_{1s} + \dot{v}_\parallel (\partial f_{1s}/\partial v_\parallel) - C_{\text{linear}}[f_{1s}] =$$

$$= - f_{0s}\Big[n_s^{-1}\, dn_s/dr + Z_s e T_s^{-1}\, d\Phi_0/dr +$$

$$+ (m_s v^2/\, 2T_s - 3/2 + Z_s e T_s^{-1}\, \Phi_1)\, T_s^{-1}\, dT_s/dr\Big]\Big(\mathbf{v}_{ds} + \mathbf{v}_E\Big)\cdot\nabla r$$

System of equations in SFINCS

$$
\begin{array}{r}
\text{Kinetic equations} \\
\langle\int d^3v f_1\rangle = 0 \\
\langle\int d^3v v^2 f_1\rangle = 0 \\
\sum_s Z_s \int d^3v f_s + \lambda = 0 \\
\langle\Phi_1\rangle = 0
\end{array}
\left\{
\begin{pmatrix}
\text{contains } \Phi_1 & & & & 0 \\
 & 0 & 0 & 0 & 0 \\
 & 0 & 0 & 0 & 0 \\
 & 0 & 0 & 0 & \\
0 & 0 & 0 & & 0
\end{pmatrix}
\begin{pmatrix}
f_1 \\ S_\mathrm{p} \\ S_\mathrm{h} \\ \Phi_1 \\ \lambda
\end{pmatrix}
=
\begin{pmatrix}
H(\Phi_1) \ \text{nonlinear} \\ 0 \\ 0 \\ K(\Phi_1) \\ 0
\end{pmatrix}
\right.
$$

Quasi-neutrality

Constraints added to make system square and eliminate null space

Sources added for steady-state solution to exist

Lagrange multiplier should come out as 0

Do we need the additional physics that SFINCS can provide?

- Calculation of C^{6+}-fluxes for the LHD impurity hole plasmas.

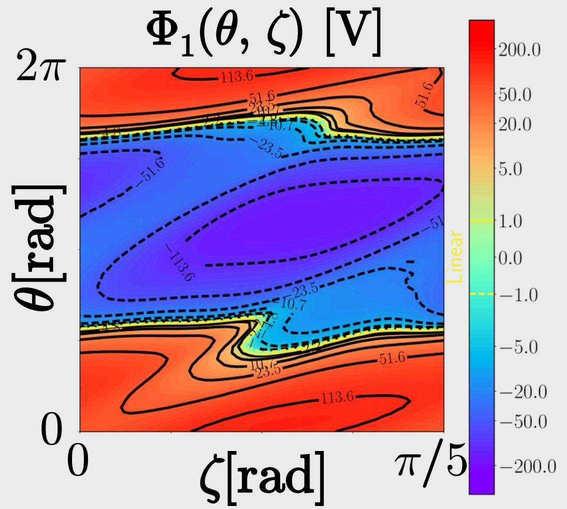

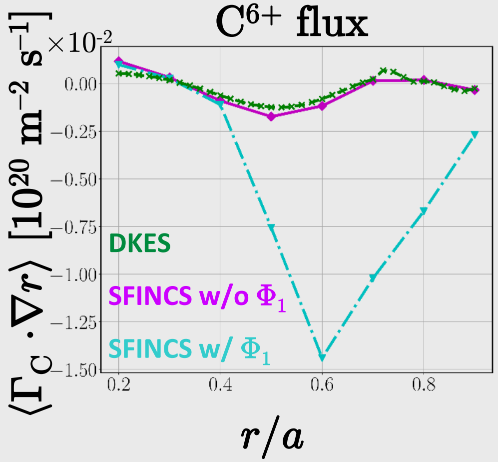

- Verify mixed-collisionality transport regime with advanced collision operator.

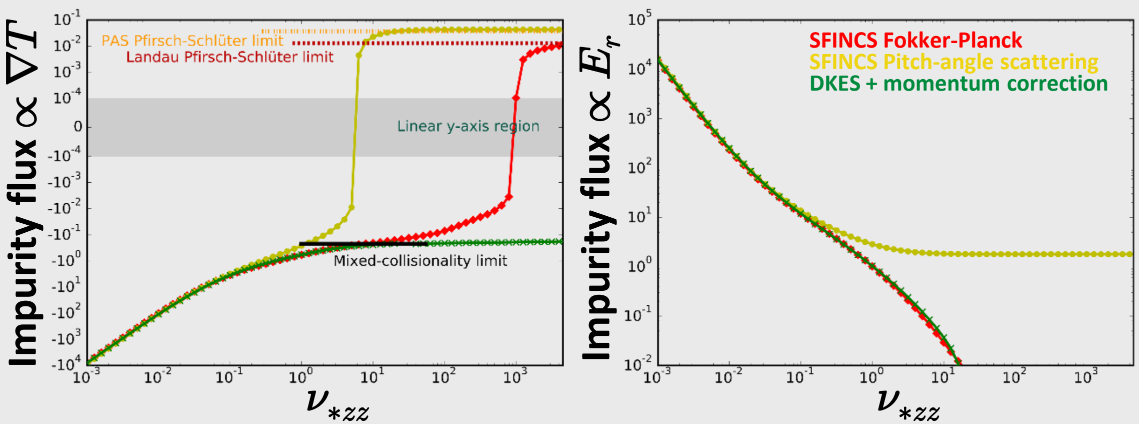

- SFINCS is more suitable than DKES in an optimization loop where equilibrium and transport calculations have to be reiterated.

- Pitch-angle scattering collisions (no momentum correction).
- Large Helical Device equilibrium (10-fold symmetry in ζ) [García-Regaña et al., Nucl. Fusion (2017)].

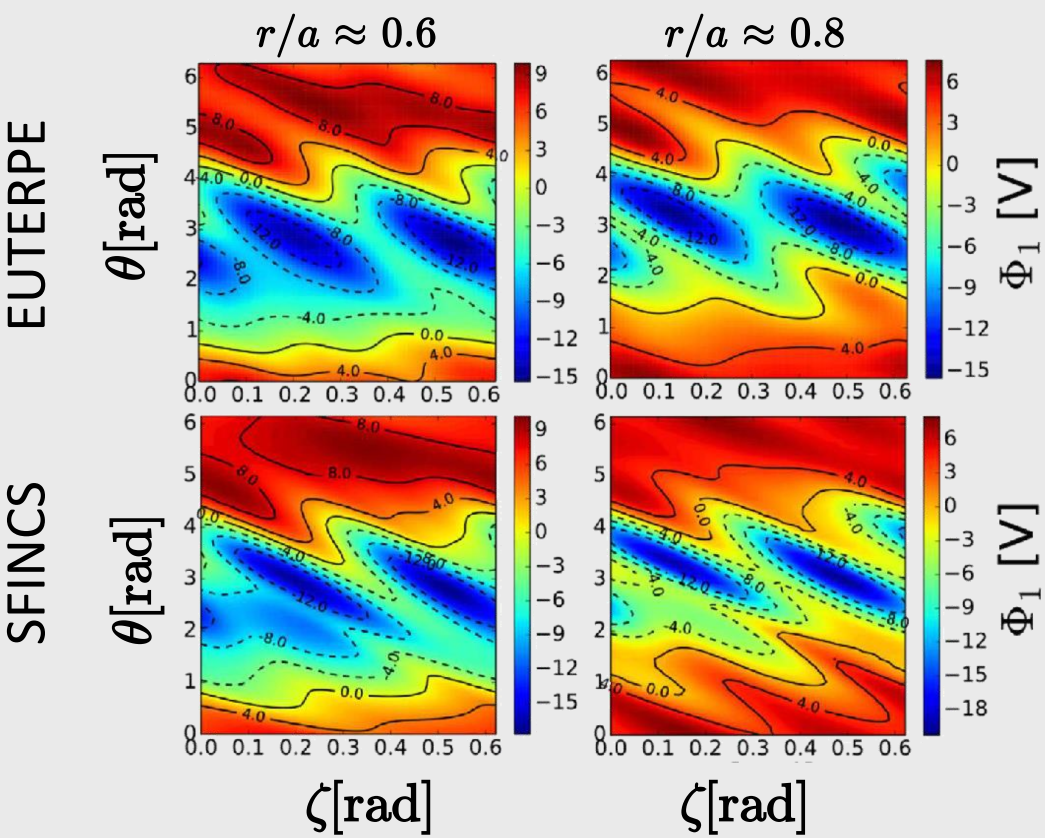

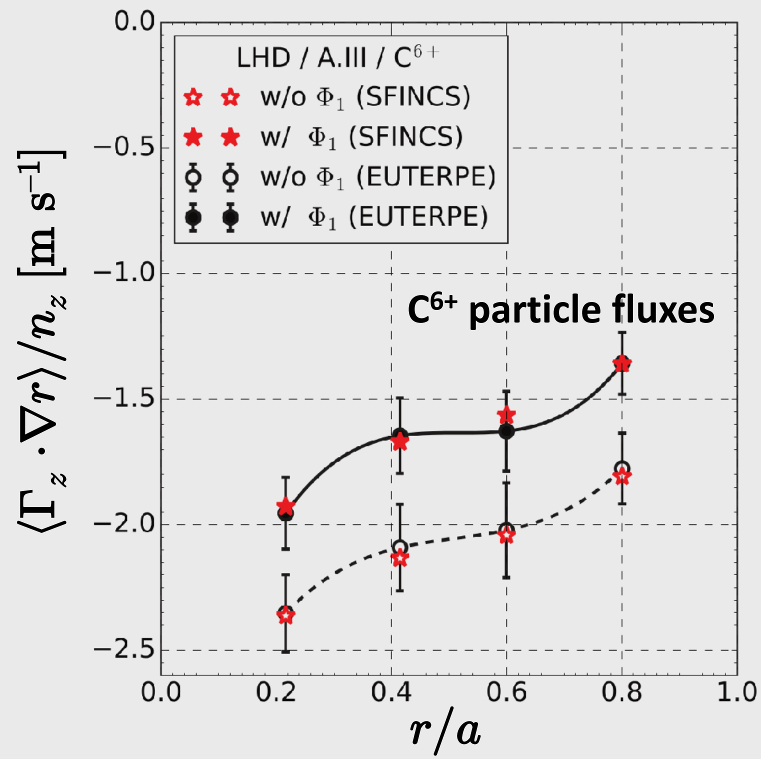

Outline

- Introduction to impurity transport in 3D plasmas
- Numerical tools and the SFINCS code
- Experimental observations of impurity transport
- Linear gyrokinetic modelling of impurity transport with equilibrium electrostatic potential variations
- Summary

The carbon impurity hole in Large Helical Device

- No accumulation of C^{6+} -impurities in LHD although all predictions of both neoclassical and turbulent transport point towards accumulation. (Inward pointing E_r).

  [Ida et al., Phys. Plasmas (2009)], [Yoshinuma et al., Nucl. Fusion (2009)].

  Assuming that external source/sink is zero (or negligible) steady density profiles should be sustained by balanced fluxes;

  $$\Gamma_c^{(\text{turb})} + \Gamma_c^{(\text{neo})} = 0$$

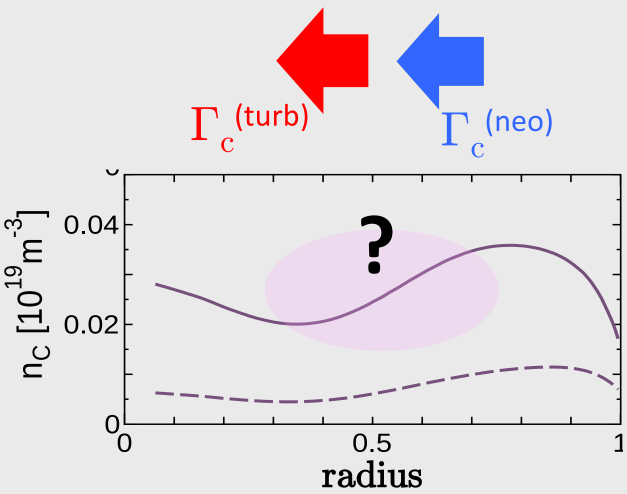

- **Still an open problem.**

  Is outward $\Gamma_c^{(\text{neo})}$ or $\Gamma_c^{(\text{turb})}$ compatible with a hollow impurity profile?

  [Nunami et al., International Stellarator-Heliotron Workshop (2017)]

- LHD deuterium experiment started March 2017.

  C^{6+} -profile more peaked in deuterium plasmas than in hydrogen plasmas.

  [Morisaki et al., International Stellarator-Heliotron Workshop (2017)]

  Isotope effect on C^{6+} transport. *Suggests that turbulent impurity transport dominates?*

Φ_1 in neoclassical transport does not seem to explain the impurity hole in LHD

- Large Helical Device discharge 113208 at t = 4.64s studied in [Nunami et al., IAEA conference (2016)], [Mikkelsen et al., Phys. Plasmas (2014)], [Velasco et al., Nucl. Fusion (2017)].
- Neoclassical particle fluxes compared to turbulent particle fluxes at steady-state.
- Direction of e^--, H^+- and He^{2+}-fluxes match; C^{6+}-fluxes do not match!
- Can Φ_1 in neoclassical calculation explain the discrepancy in the C^{6+}-fluxes?
- **SFINCS calculations:**
  - Φ_1 can vary strongly on flux-surface: ± 200 V.
  - Φ_1 has large impact on C^{6+}-fluxes, but in wrong direction to explain hollow C^{6+}-profile.

[Mollén et al., PPCF (2018)]

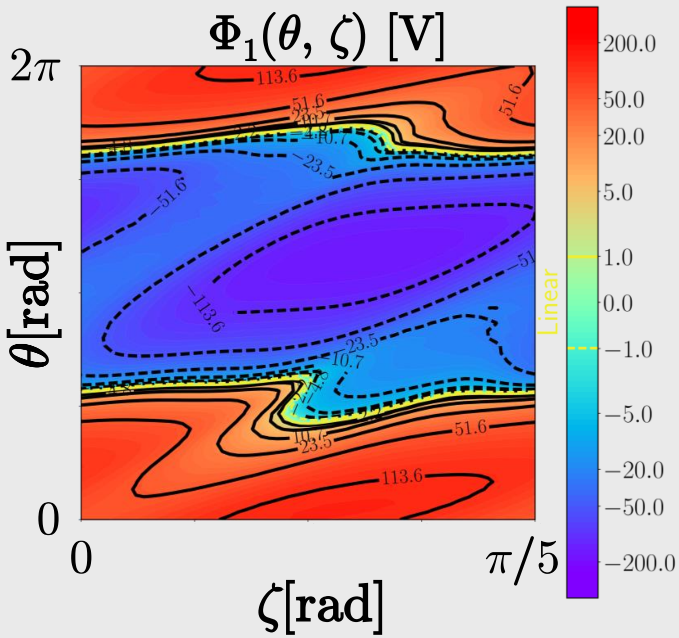

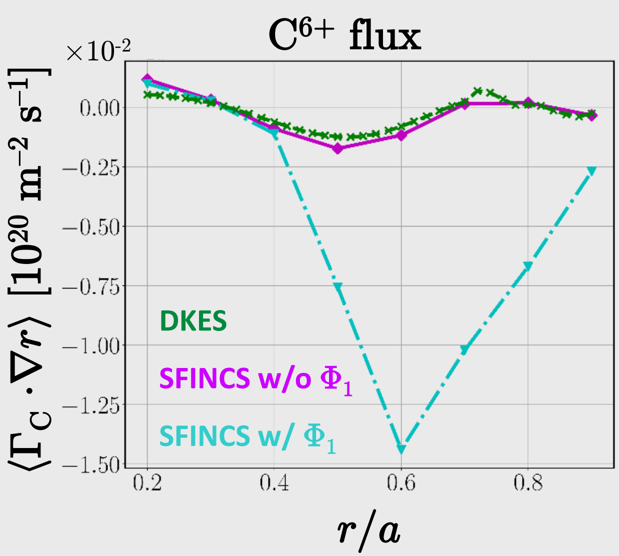

Is impurity transport neoclassical in optimized stellarators?

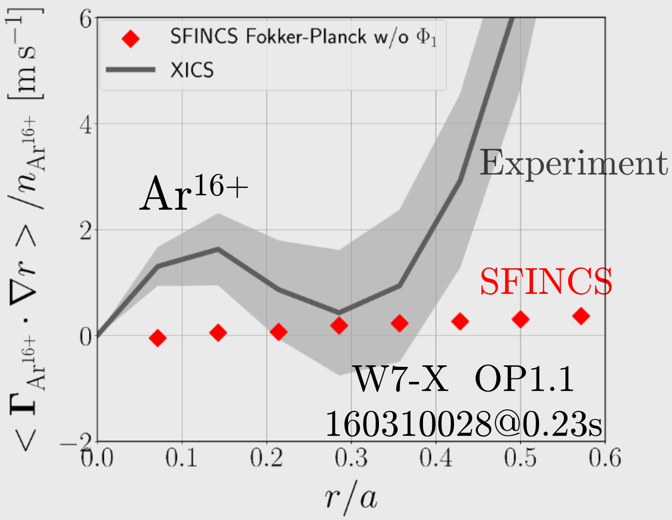

- Wendelstein 7-X OP1.1 →

  Ongoing work to analyze OP1.2 plasmas.

- Wendelstein 7-X OP1.2a:

  Iron analyzed by VUV and x-ray spectrometers.

  STRAHL + DKES modelling.

  "Anomalous diffusion profile two orders of magnitude larger than the neoclassical".

  [Geiger et al., Nucl. Fusion (2019)]

- Nonlinear gyrokinetic flux-tube simulations in LHD with the GKV code find an order of magnitude larger C^{6+}-fluxes than neoclassical calculations. [M. Nunami & M. Nakata]

- Only a few gyrokinetic studies of turbulent impurity transport in stellarators exist:

  [Mikkelsen et al., PoP (2014)], [Nunami et al., IAEA (2016)], [Helander & Zocco, PPCF (2018)]

- Perhaps Φ_1 can play a role also in turbulent impurity transport.

Radial impurity flux $\langle \Gamma_z \cdot \nabla r \rangle = -\, D_z \, dn_z/dr + V_z \, n_z$

- Size of the convective velocity V_z is consistent with neoclassical calculations for W7-X, but neoclassical diffusion D_z is orders of magnitude too low to explain experimental observations.

- Impurity confinement time τ_I independent of Z within experimental uncertainties.

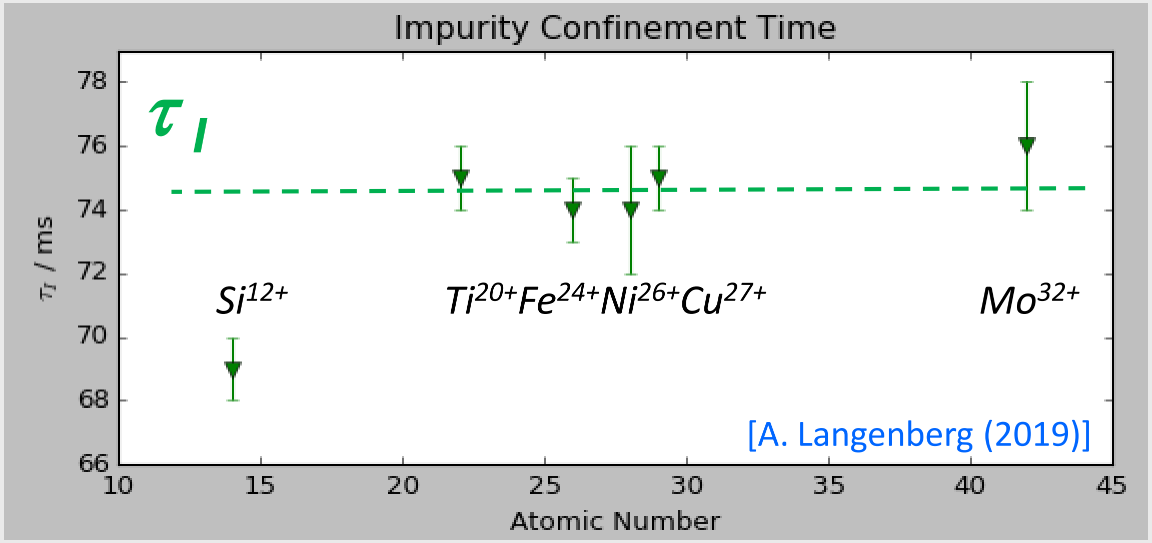

- Hypothesis: The radial impurity transport is dominated by turbulent transport, which to lowest order is
  - independent of Z and m_z,
  - independent of E_r,
  - dominated by diffusion. [Helander & Zocco, PPCF (2018)]

- Neoclassical analysis with EUTERPE and SFINCS is ongoing.

Outline

- Introduction to impurity transport in 3D plasmas
- Numerical tools and the SFINCS code
- Experimental observations of impurity transport
- Linear gyrokinetic modelling of impurity transport with equilibrium electrostatic potential variations
- Summary

Effect of Φ_1 on quasilinear impurity fluxes (ongoing work)

- Non-fluctuating potential $\Phi_1(\theta, \zeta) = \Phi - \Phi_0(\psi); \quad \Phi_0(\psi) = \langle\Phi\rangle; \quad \Phi_1 \ll \Phi_0$

- Energy is $\varepsilon = m_s v^2/2 + Z_s e\, \Phi_1(\theta, \zeta) + Z_s e\, \phi(t, \theta, \zeta)$

  $\Phi_1(\theta, \zeta)$ - equilibrium potential

  $\phi(t, \theta, \zeta)$ - fluctuating potential

Note: Turbulent transport automatically ambipolar to lowest order, independent of $E_r = -d\Phi_0/dr$

$\Rightarrow$ Φ_0 can be transformed away.

- Lowest order distribution $f_{0s} = f_{Ms} \exp(-Z_s e \Phi_1/T_s)$

  $f_{Ms} = n_{0s}(\psi)\ (m_s v^2/2\pi T_s)^{3/2} \exp(-m_s v^2/2T_s)$ Maxwellian.

- $\Phi_1(\theta, \zeta)$ is obtained from a neoclassical calculation with a code like SFINCS.

  In our gyrokinetic model $\Phi_1(\theta, \zeta)$ is an input.

Effect of Φ_1 on quasilinear impurity fluxes

- Linear gyrokinetic equation for the non-adiabatic distribution g_s

$$f_s = f_{0s}\,(1 - Z_s e\,\phi/T_s) + g_s$$

$$v_\| \nabla_\| g_s - i\,(\omega - \omega_E - \omega_{ds})\; g_s = C\,[g_s] - i\;(Z_s e\;\phi/T_s)\;J_0(k_\perp v_\perp/\Omega_s)\;f_{0s}\;(\omega - \omega^T{}_{\star s})$$

$\omega = \omega_r + i\gamma$ mode frequency

$\alpha = q(\psi)\;\theta - \zeta$

$\mathbf{k}_\perp = k_\alpha \nabla\alpha + k_\psi \nabla\psi \approx k_\alpha \nabla\alpha$

$\omega_E = \mathbf{v}_{\Phi_1}\cdot\,\mathbf{k}_\perp = (k_\alpha/B)\;(\mathbf{b}\times\nabla\Phi_1)\,\cdot\,\nabla\alpha$ (usually ignored because small for i, e)

$\omega_{ds} = \mathbf{v}_{ds}\cdot\,\mathbf{k}_\perp = k_\alpha\;[\mathbf{b}\times(v_\perp{}^2\,\nabla\,\ln B/2 + v_\|{}^2\;\boldsymbol{\kappa})/\;\Omega_s]\,\cdot\,\nabla\alpha$

$\omega^T{}_{\star s} = -\;(T_s/Z_s eB) f_{0s}{}^{-1}\;(\mathbf{b}\,\times\,\mathbf{k}_\perp)\,\cdot\,\nabla(f_{0s})_\varepsilon = \omega_{\star s}\;q\;[1 + \eta_s(m_s v^2/\;2T_s - 3/2 + Z_s e T_s^{-1}\,\Phi_1)]$

$\omega_{\star s} = (k_\alpha T_s/Z_s e)\;d\;\ln n_{0s}/d\psi;$ $\eta_s = (d\;\ln T_s/d\psi)\;/\;(d\;\ln n_{0s}/d\psi)$

We neglect parallel streaming $v_\| \nabla_\| g_s$ and collisions $C\,[g_s]$.

Effect of Φ_1 on quasilinear impurity fluxes

- The $E\times B$ drift frequency ω_E usually neglected because it is small, unless $Z_s e\Phi_1/T_s \sim \mathcal{O}(1)$.

- Note that ω_E independent of Z_s, whereas

  $\omega_{ds} \sim 1/Z_s$

  $\omega^T{}_{\star s} \sim 1/Z_s$.

  $\Rightarrow$ for high-Z impurities ω_E could play a role.

- The flux-surface-averaged quasilinear impurity flux is given by

  $$\Gamma_z = - k_\alpha \, \mathrm{Im} \left[\left\langle \int g_z J_0 \phi^* \, \mathrm{d}^3 v \right\rangle \right]$$

  and we find that

  $$\Gamma_z = - (Ze/T_z) \; k_\alpha \, \gamma \left\langle |\phi|^2 \int (\omega^T{}_{\star z} - \omega_E - \omega_{dz}) \; |\omega - \omega_E - \omega_{Dz}|^{-2} \; J_0{}^2 \; f_{0z} \, \mathrm{d}^3 v \right\rangle$$

  which implies that Φ_1 can only change the sign of Γ_z if it can change the sign of $(\omega^T{}_{\star z} - \omega_E - \omega_{dz})$.

Effect of Φ_1 on quasilinear impurity fluxes

- To perform the velocity integral we assume:
  - Low-β plasma $\Rightarrow$ simplify ω_{dz} using $\boldsymbol{\kappa} \approx \nabla_\perp B/B$:
    $\omega_{dz} = \omega_B\ (v_\perp{}^2\ /\ 2 + v_\parallel{}^2)\ /\ v_z{}^2$
  - Ion-scale turbulence $\Rightarrow k_\perp{}^2\rho_z{}^2/2 \ll 1$.
  - High-Z trace impurities so ω obtained from bulk species gyrokinetic equations.
  - Order ω_E/ω, ω_{dz}/ω, $\omega^T{}_{\star z}/\omega$ and $J_0(k_\perp v_\perp/\Omega_z)$ - 1 as $1/Z$ small quantities.

- Use Boozer coordinates $\mathbf{B} = \mathrm{H}(\psi, \theta, \zeta)\ \nabla\psi + \mathrm{I}(\psi)\ \nabla\theta + \mathrm{G}(\psi)\ \nabla\zeta$.

- $\Gamma_z \simeq$ - $(Ze/T_z)\ k_\alpha\ [\gamma/(\omega_r{}^2 + \gamma^2)]\ n_{0z}(\psi)\ q\ \omega_{\star z}\ \big\langle|\phi|^2 \exp(\text{-}Z_s e\Phi_1/T_s)\ \big\{1 + \eta_z\ ZeT_z^{-1}\ \Phi_1$
  - $\omega_E/(q\ \omega_{\star z})$ - $\omega_B\ /(q\ \omega_{\star z})\big\}\big\rangle =$
  - $k_\alpha{}^2\ [\gamma/(\omega_r{}^2 + \gamma^2)]\ (dn_{0z}/d\psi)\ q\ \big\langle|\phi|^2 \exp(\text{-}Z_s e\Phi_1/T_s)\ \big\{\boldsymbol{1 + \eta_z\ ZeT_z^{-1}\ \Phi_1}$
  $+ (Ze/T_z)\ (\mathrm{d}\ln n_{0z}/d\psi)^{-1}\ (q\ \mathrm{G} + \mathrm{I})^{-1}[\mathrm{H}\ (q\ d\Phi_1/d\zeta + d\Phi_1/d\theta) + \theta\ dq/d\psi\ (\boldsymbol{\mathrm{G}d\Phi_1/d\theta}$ - $\mathrm{I}d\Phi_1/d\zeta)]$
  $+ (2/B)\ (\mathrm{d}\ln n_{0z}/d\psi)^{-1}\ (q\ \mathrm{G} + \mathrm{I})^{-1}[\mathrm{H}\ (q\ dB/d\zeta + dB/d\theta) + \theta\ dq/d\psi\ (\boldsymbol{\mathrm{G}dB/d\theta}$ - $\mathrm{I}dB/d\zeta)]$
  - $(2/B)\ (\mathrm{d}\ln n_{0z}/d\psi)^{-1}\ dB/d\psi$ $\big\}\big\rangle$

Dominant terms

Effect of Φ_1 on quasilinear impurity fluxes

- Using $\mathbf{B} = \mathrm{H}(\psi,\, \theta,\, \zeta)\, \nabla\psi + \mathrm{I}(\psi)\, \nabla\theta + \mathrm{G}(\psi)\, \nabla\zeta$ with

  $\mathrm{G} \gg \mathrm{I}$ (poloidal current outside flux-surface $\gg$ toroidal current inside flux-surface).

  $|\mathrm{H}\ \nabla\psi|/(\mathrm{G}|\nabla\psi|) \sim (\beta\Delta B/B)/(r/R_0) \ll 1 \Rightarrow$ neglect H/G terms.

$$\Gamma_z \simeq - k_\alpha^2\, [\gamma/(\omega_r^2 + \gamma^2)]\, (dn_{0z}/d\psi)\, q\, \Big\langle |\phi|^2 \exp(-Z_s e \Phi_1/T_s)\, \Big\{1 + \eta_z\, ZeT_z^{-1}\, \Phi_1 +$$
$$(d\ln n_{0z}/d\psi)^{-1}\, \theta q^{-1} dq/d\psi\, (Ze/T_z) d\Phi_1/d\theta + (2/B)(d\ln n_{0z}/d\psi)^{-1}\, \theta q^{-1} dq/d\psi\, dB/d\theta - (2/B)(d\ln n_{0z}/d\psi)^{-1} dB/d\psi \Big\}\Big\rangle.$$

- What is the physics behind the $\eta_z\ ZeT_z^{-1}\, \Phi_1$ term?

  Real lowest-order density $N_{0z}(\psi,\, \theta,\, \zeta) = n_{0z}(\psi)\, \exp(-Z_z e\Phi_1/T_z) \Rightarrow$

  $d\ln N_{0z}/d\psi = (d\ln n_{0z}(\psi)/d\psi)\, (1 + \eta_z\, ZeT_z^{-1}\, \Phi_1)$

  varies over the flux-surface with Φ_1.

- **The most important is $d\ln N_{0z}/d\psi$ where the turbulence is located!**

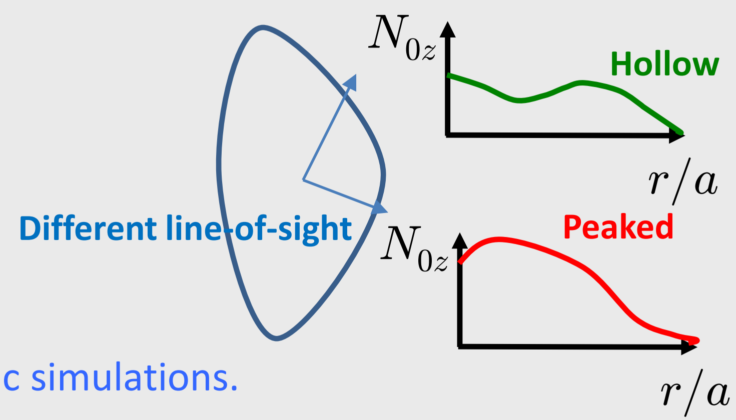

- Next step: Attempt to include $\Phi_1(\theta,\, \zeta)$ in linear gyrokinetic simulations.

- Introduction to impurity transport in 3D plasmas
- Numerical tools and the SFINCS code
- Experimental observations of impurity transport
- Linear gyrokinetic modelling of impurity transport with equilibrium electrostatic potential variations
- Summary

Summary

- Collisional (neoclassical) transport predictions for stellarators have long been based on simplified models, but numerical tools start appear that can advance our understanding.

- The SFINCS code can simultaneously investigate several new effects:
  - Multi-species calculations with non-adiabatic electrons and non-trace impurities.
  - Full linearized Fokker-Planck-Landau operator.
  - Self-consistent calculation of the ambipolar radial electric field.
  - Calculations including electrostatic potential variations $\Phi_1\,(\theta,\,\zeta)$.

- These effects can be important in calculations of impurity transport.

- Initial analysis of Wendelstein 7-X plasmas indicate that the impurity transport is dominated by anomalous diffusion.

- Gyrokinetic modelling/calculations of turbulent impurity transport in stellarators is at an early stage, but will hopefully make progress in the coming years.

Extra slides

SFINCS implementation and numerical details

- Eulerian uniform grid in θ, ζ.

  MPI parallelization with PETSc library + MUMPS.

- Spectral discretization in $\xi = v_{\|}/v$: Legendre polynomials $P_{\mathrm{n}}(\xi)$.

- Spectral collocation discretization for $x = v/v_{Ts}$, non-standard orthogonal polynomials [Landreman & Ernst, J Comput. Phys. (2013)].

  Collocation: function is known on a set of grid points rather than explicitly expanded in a set of modes $\Rightarrow$ integration/differentiation weight matrices.

- Non-linear system solved with Newton method:

  $\mathbf{x} = (f_1, \Phi_1)$ Residual $R(\mathbf{x}) = 0$ Jacobian $R' = \delta R(\mathbf{x})/\delta\mathbf{x}$

  State-vector updated as $\mathbf{x}_{n+1} = \mathbf{x}_n - R(\mathbf{x}_n)/R'(\mathbf{x}_n)$.

- System solved using preconditioned GMRES.

- Code written in Fortran (also MATLAB version).

SFINCS numerical resolution, expensive simulations at low collisionality

- Trapped-passing boundary (tokamak example):

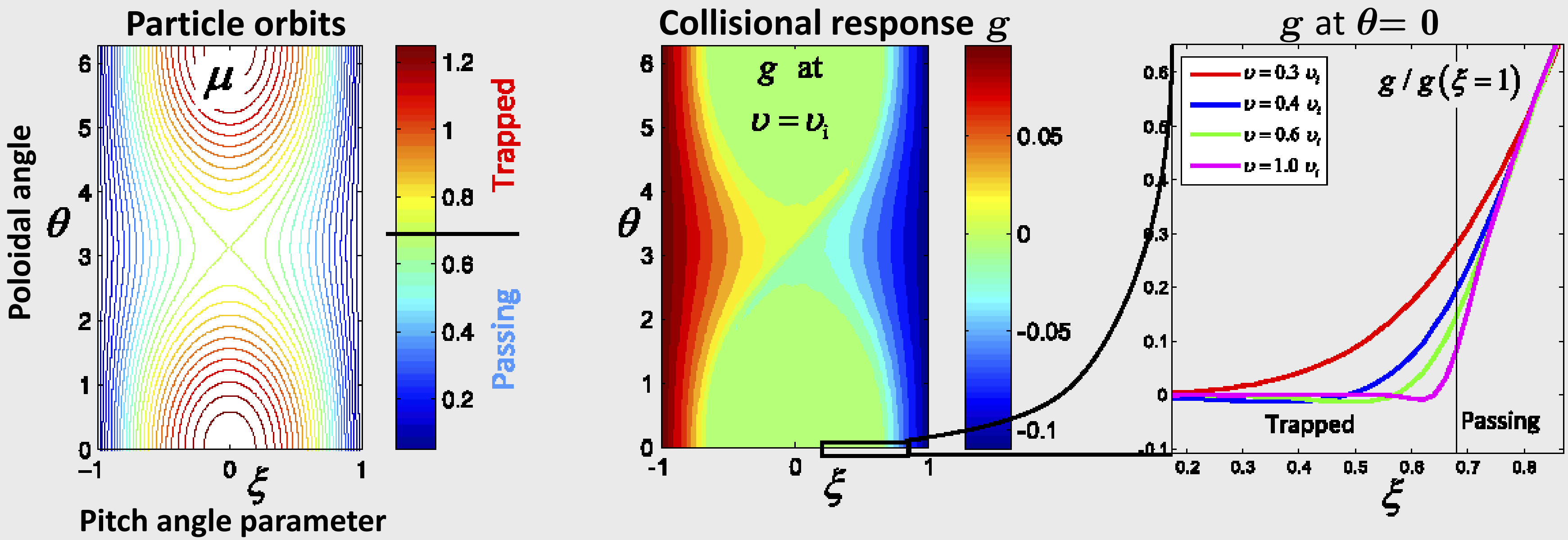

- Simulations typically become more demanding at low collisionality (small ν_{ss}/v_{Ts}). Thinner trapped-passing boundary layer harder to resolve.

- Resolution in SFINCS runs for W7-X OP1.1:
$(N_{\text{species}} \times N_\theta \times N_\zeta \times N_x \times N_\xi) \times (N_{\text{species}} \times N_\theta \times N_\zeta \times N_x \times N_\xi) \sim 10^7 \times 10^7$
Runs on IPP Draco cluster $\leq$ 32 nodes (128GB) in ≤ 20 min (often ≤ 5 min).

- Most time consuming activities: - find numerical convergence,
- find ambipolar E_r .

Can we trust that SFINCS is correct?

SFINCS can perform calculations that no other code can (to my knowledge).

Benchmark of linear calculations

- Comparison to analytic limits at high-collisionality $\nu_{*ii} \sim \nu_{ii}/v_{Ti} \gg 1$.
  Comparison to analytic theory at mixed-collisionality $\nu_{*zz} \gg 1;\ \nu_{*ii} \ll 1$.

- Comparison to DKES and EUTERPE for transport calculations.
  Note: A wider benchmark activity would be desirable.

Benchmark of nonlinear calculations including Φ_1

- Comparison between Fortran version of SFINCS with Φ_1 (equations included by me) and Matlab version (written by Matt) .

- Some sanity checks in the output of SFINCS, e.g. $\langle \Gamma_s \cdot \nabla r \rangle = \langle \int d^3v f_{0s} (\mathbf{v}_{ds} + \mathbf{v}_E) \cdot \nabla r \rangle = 0$.

- Benchmark with EUTERPE, KNOSOS for several plasmas.

Additional features implemented in SFINCS (ongoing work)

- Φ_1 in collision operator.

$$C_{ab}{}^{\text{linear}}[f_s] = C_{ab}[f_{\text{M}a},\ f_{\text{M}b}]\ \exp(\text{-}Z_a e\Phi_1/T_a\ \text{-}Z_b e\Phi_1/T_b) +$$
$$+\ C_{ab}[f_{1a},\ f_{\text{M}b}]\ \exp(\text{-}Z_b e\Phi_1/T_b) + C_{ab}[f_{\text{M}a},\ f_{1b}]\ \exp(\text{-}Z_a e\Phi_1/T_a)$$

- Linear version with Φ_1.

  Version of the code where Φ_1 is an input instead of an output.

  Could be useful e.g. for studying effect of plasma heating or using Φ_1 from another code.

- Φ_1 + tangential magnetic drifts.

  Found to be important for some plasmas.

  [Velasco et al., PPCF (2018)], [Calvo et al., PPCF (2017); Nucl. Fusion (2018)]

Φ_1 + tangential magnetic drifts

Drift-kinetic equation

$$\begin{cases} \dot{\mathbf{R}} = v_\parallel \mathbf{b} - (\nabla\Phi_0 \times \mathbf{b})/B + \mathbf{v}_{ds}\cdot\nabla f_{1s} \\ \dot{v}_\parallel = - Z_s e \mathbf{b}\cdot\nabla\Phi_1/m_s - \mu \mathbf{b}\cdot\nabla B - v_\parallel (\mathbf{b}\times\nabla B)\cdot\nabla\Phi_0/B^2 \end{cases}$$

extra term containing tangential magnetic drifts, drop terms with radial coupling to keep locality

$$\dot{\mathbf{R}}\cdot\nabla f_{1s} + \dot{v}_\parallel(\partial f_{1s}/\partial v_\parallel) - C_{\text{linear}}[f_{1s}] =$$

$$= - f_{0s}\big[n_s^{-1}\, dn_s/dr + Z_s e T_s^{-1}\, d\Phi_0/dr +$$

$$+ (m_s v^2/\, 2T_s - 3/2 + Z_s e T_s^{-1}\,\Phi_1)\; T_s^{-1}\, dT_s/dr\big]\big(\mathbf{v}_{ds} + \mathbf{v}_E\big)\cdot\nabla r$$

- Magnetic drifts implemented in SFINCS [Paul et al., Nucl. Fusion (2017)].
- To include tangential magnetic drifts in a numerical solver is somewhat ambiguous.
  Example: Approximation $df_{1s}/dr = 0$ in $\mathbf{v}_{ds}\cdot\nabla f_{1s}$ different in different coordinate systems.
- 9 different versions implemented in SFINCS.
- SFINCS calculations with Φ_1 + tangential magnetic drifts very numerically challenging.
- KNOSOS significantly faster. [Velasco et al., PPCF (2018)]

Benchmark EUTERPE, SFINCS, KNOSOS

- Pitch-angle scattering collisions (no momentum correction).
- Large Helical Device equilibrium.
- Tangential magnetic drifts.

Without tangential magnetic drifts

With tangential magnetic drifts

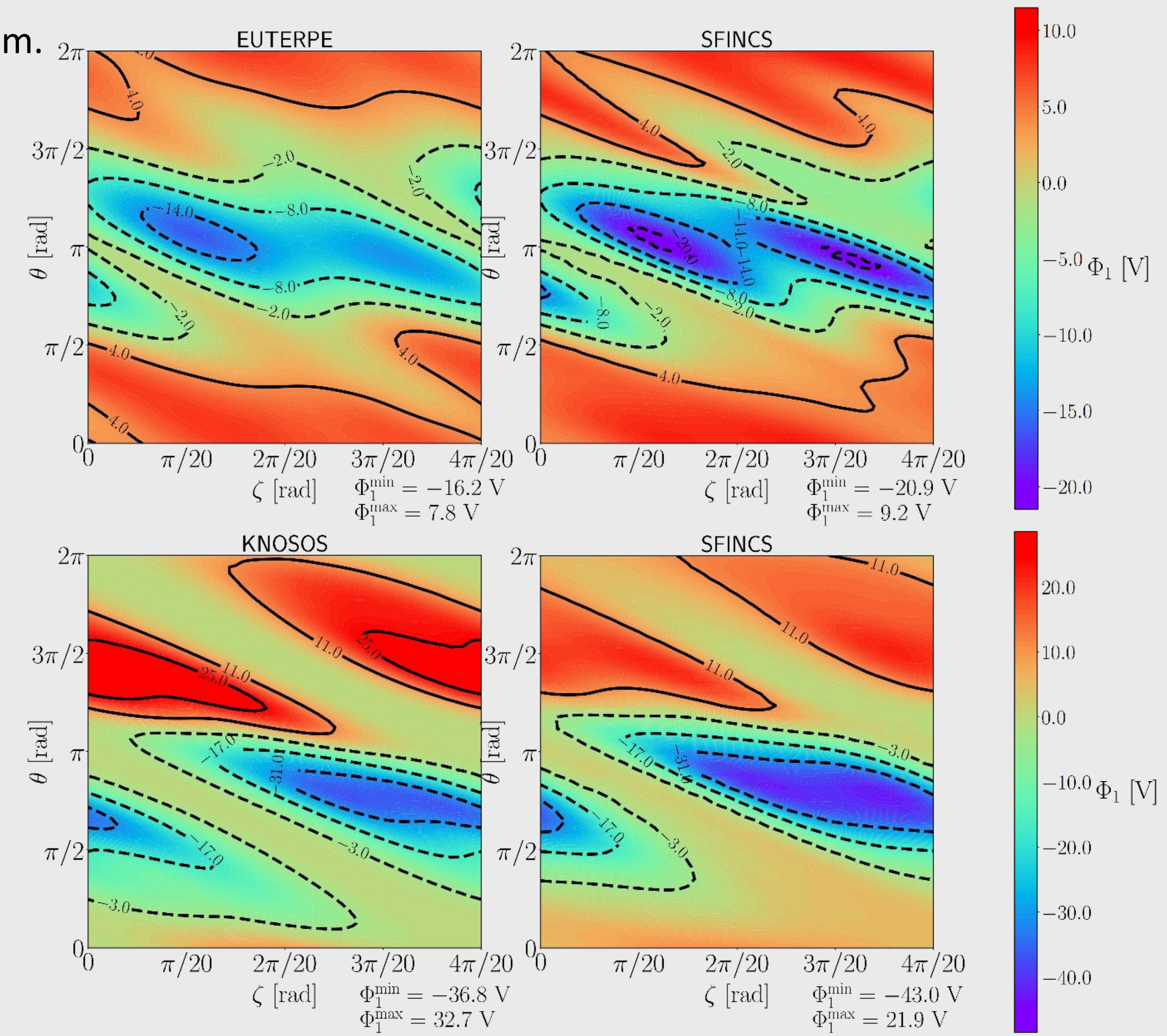

Can effect of Φ_1 on quasilinear impurity fluxes explain the impurity hole in LHD?

Large Helical Device

10-periodic in toroidal direction

Bad curvature $L2$

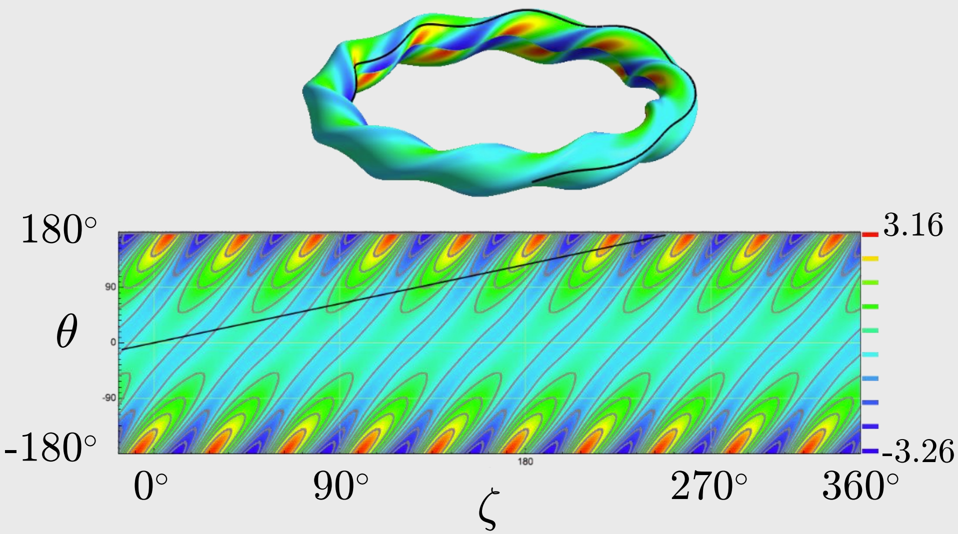

Metric coefficient $g^{11} = |\nabla\psi|^2$

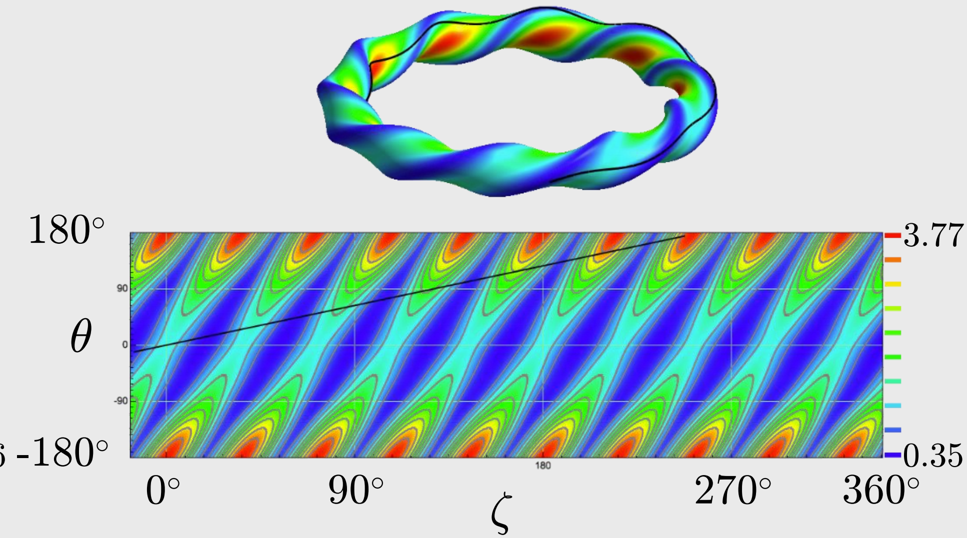

- Most probable location for turbulence is areas on outboard side between ridges (around $\theta = 0$, $\zeta = 0$). There $L2 < 0$ (bad curvature) and g^{11} is maximized $\Rightarrow$ optimal conditions for turbulence.
- Approximate $|\phi|^2$ with 2D parabola around $\theta = 0$, $\zeta = 0$.

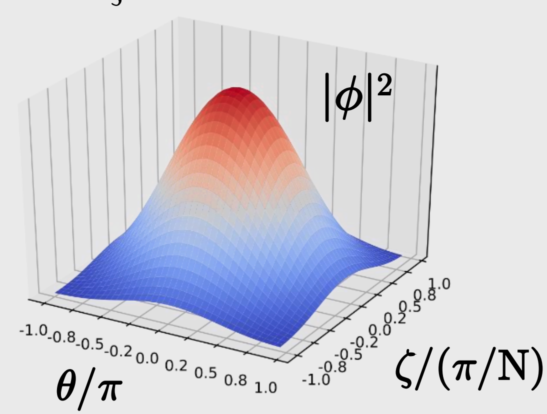

Can effect of Φ_1 on quasilinear impurity fluxes explain the impurity hole in LHD?

- Large Helical Device discharge 113208 at t = 4.64s

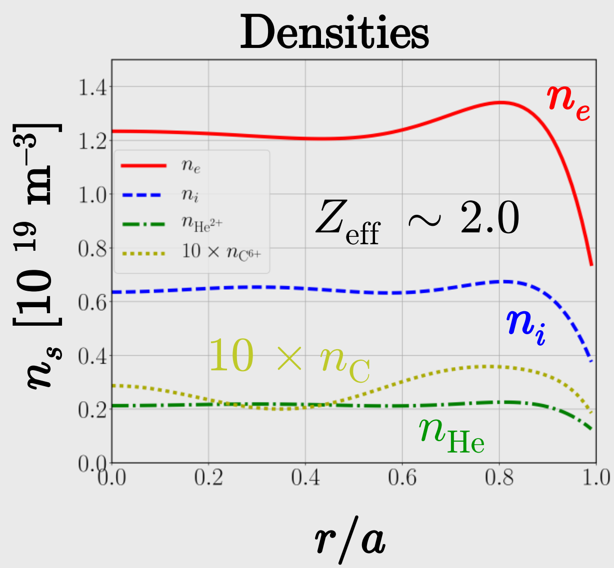

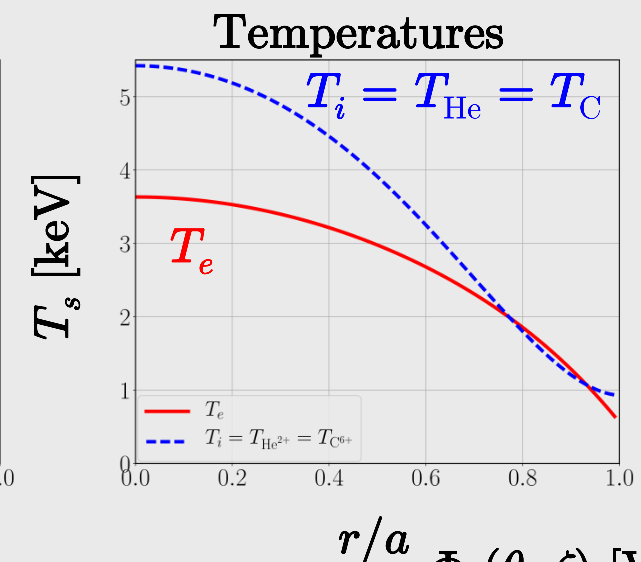

- Look at $r/a = 0.7$, hollow density profile,

  $\eta_z = (d\ \ln T_z/d\psi)\ /\ (d\ \ln n_{0z}/d\psi) =$ -3.5,

  $\Phi_1(0,\ 0) = 34.5$ V,

  $\eta_z\ ZeT_z^{-1}\ \Phi_1(0,\ 0) =$ -0.29.

- $\eta_z\ ZeT_z^{-1}\ \Phi_1$ seems to contribute to outward Γ_z.
- Maybe not enough to explain impurity hole but a more careful analysis is needed.

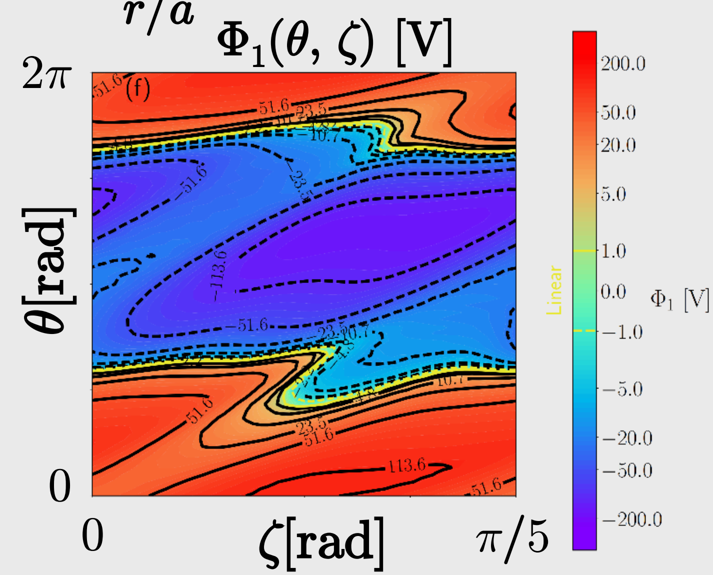

Further ideas on quasilinear impurity fluxes

Effect of Φ_1 could possibly change by:

- Tangential magnetic drifts included in the SFINCS calculations (or Φ_1 from KNOSOS).
- Including effects of plasma heating.
- Include parallel streaming term.

  Axisymmetry: Trapped Electron Modes $\Rightarrow$ outwards transport,

  Ion Temperature Gradient modes $\Rightarrow$ inwards transport.

- Including radial variation $\Phi_1(\psi, \theta, \zeta)$, requires radially global neoclassical code but including $d\Phi_1/d\psi$ in the quasilinear model should be straightforward.